ELSEVIER

Chemical Engineering Journal 130 (2007) 179–185

Chemical Engineering Journal

www.elsevier.com/locate/cej

Analysis of bubble behaviors in bubble columns using electrical resistance tomography

H. Jin [a,*], M. Wang [b], R.A. Williams [b]

[a] *School of Materials and Chemical Engineering, Beijing Institute of Petrochemical Technology, Beijing 102617, PR China*
[b] *Institute of Particle Science & Engineering, School of Process, Environmental and Materials Engineering, University of Leeds, Leeds LS2 9JT, UK*

Abstract

The distribution of gas holdup, the rise velocity of gas bubble swarm and the Sauter mean bubble size are estimated with a small diameter laboratory scale bubble column using electrical resistance tomography (ERT). The theory of gas disengagement based on ERT methods has been developed for estimations of bubble size and bubble rise velocity. The gas holdups of large bubble swarm and small bubble swarm, the distribution of both bubble size are derived through the analysis of gas disengagement based on the differences of the rise velocity of bubble swarm at the cross-section imaged by electrical resistance tomography. Experimental results are in very good agreement with correlations and conventional estimation obtained using pressure transmitter methods. The proposed methodology can be also used as an analysis tool for quantifying and optimizing the performance of other types of complex reaction systems.

Keywords: Bubble column; Bubble behavoir; Electrical resistance tomography; Gas holdup

1. Introduction

Bubble columns are widely used as gas–liquid contacting devices due to their ease of operation and ability to enable good gas/liquid mixing and high heat transfer rates in a controlled manner [1]. However, the sophisticated industrial applications demand deep knowledge of the fundamental behavior of such systems in order to improve process efficiency [2].

Bubbles swarm characters, such as gas holdup, bubble size and bubble rise velocity, affect the specific gas–liquid interfacial area, resident time distribution, transfer rates and reaction rates in chemical processes. Therefore, the bubble behavior plays an important role in designing and scaling-up the bubble column reactors. In order to determine the specific gas–liquid interfacial area, an accurate measurement on bubble size distribution is required. The technique of dynamic gas disengagement (DGD) is very widely adopted method to study gas holdup, bubble size and bubble rise velocity. The technique was firstly introduced by Sriram and Mann [3], based on the disengagement-rates of the gas holdup and level of gas–liquid dispersion after the gas flow to the bubble column was shut off. Several researches further developed the method to understand the complex mechanisms of hydrodynamics. Krishna et al. [4] and Maretto and Krishna [5] found that bubbles were divided into two sorts of large bubbles and small bubbles according to the rise velocity of the bubbles and the different sizes of the bubbles resulted in the different dynamic characteristics during the bubbles rose in the column. Shetty et al. [6] studied the back-mixing in the bubble column using a two-bubble class hydrodynamic model, and their calculated results were in good agreement with the experimental data. Patel et al. [7] measured the size of the bubble using both photography technique and dynamic gas disengagement method, whose results showed that systems having similar physical properties had vastly different gas holdups and bubble size distributions.

Electrical resistance tomography (ERT) has been introduced and used in various industrial investigations for visualization of the concentration profiles and characteristics of the fluid dynamics in gas–liquid two-phase systems [8–10]. Many investigations have been carried out using electrical resistance tomography in bubble columns. Fransolet et al. [11,12] studied the gas holdup and the qualitative diagnosis of sparger functioning in a bubble column. Meanwhile, the effect of theological properties of the liquid on gas holdup using ERT and DGD have been presented. Wang et al. [13] developed a new method for identification of flow in a bubble column using electrical resistance tomography. Toye et al. [14] examined the potentialities of an electrical resistance tomography device, and found that variable gas flow rate determined the time resolution of the ERT in a bubble column.

* Corresponding author. Tel.: +86 10 81292074; fax: +86 10 69241846.
E-mail address: jinhaibo@bipt.edu.cn (H. Jin).

1385-8947/$ – see front matter © 2006 Elsevier B.V. All rights reserved.
doi:10.1016/j.cej.2006.08.032

Nomenclature

d_b	bubble diameter (mm)
d_s	Sauter mean bubble size (mm)
D_T	column diameter (m)
g	gravitational constant (m s^{-2})
H	vertical distance above the gas distributor (m)
H_1, H_2	the ERT sensing planes 1 and 2 vertical distance above the gas distributor (m)
t	time (s)
u_b	bubble rise velocity (cm s^{-1})
$\bar{u}_b$	mean bubble rise velocity (cm s^{-1})
u_g	gas superficial velocity (cm s^{-1})
u_L	liquid phase velocity (cm s^{-1})

Greek letters

ε_g	gas holdup
μ_L	liquid viscosity (Pa s)
ν_L	liquid kinematic viscosity (m^2 s^{-1})
ρ_g	gas density (kg m^{-3})
ρ_L	liquid density (kg m^{-3})
σ_{mc}	the local mixture conductivity (mS cm^{-1})
σ_L	surface tension (N m^{-1})
σ_1	the conductivity of the first phase (mS cm^{-1})
σ_2	the conductivity of the second phase (mS cm^{-1})

Jin et al. [15] presented the effect of sparger geometry on gas bubble flow behaviors in a small bubble column using electrical resistance tomography. Electrical resistance tomography is a fast imaging technique but with low spatial resolution, which estimates the gas holdup based on boundary voltage measurements. The aim of this study is to develop a new method for estimating the bubble rise velocity and bubble size based on the electrical resistance tomography coupled with dynamic gas disengagement methods. Meanwhile, results compared with those obtained from conventional pressure transmitter and correlation methods are also reported in the paper.

2. Theory

2.1. Dynamic gas disengagement for ERT

Daly et al. presented a detailed discussion on the theory of the dynamic gas disengagement technique [16]. The principle was based on the disengagement-rates of the gas holdup and level of gas–liquid dispersion after the gas flow to the bubble column was shut off. In their model, bubbles in bubble column can be divided into a multi-modal distribution shown in Fig. 1(a). It should be pointed out that the distribution is not been really districted among the inter-bubbles and is only used for the aim of analysis. The initial state of dispersion is depicted in Fig. 1(b), whereas, $i = 1$ corresponds to the first period of disengagement ('larger' bubble engagement process). The periods of disengagement after the gas flow to the bubble column is shut off can be divided up to N (whereas $i = N$ corresponds to the last period ('smaller' bubble engagement process). Four points of the basic assumptions in the analysis were given as: (1) the dispersion is axially homogeneous at $t = 0$ (at the time of shut off the gas flow); (2) there is no bubble interaction; (3) a constant rate of disengagement process; (4) the bubble rise velocity, $u_{b,i}$, is a constant across the sectional area.

Fig. 2 shows the transient gas holdup, ε_g, which was obtained using ERT. Through Maxwell's relationship between the transient conductivity values and time, the disengagement profiles are plotted as holdup (ε_g) versus time (t) in Fig. 2(a). Meanwhile, the visualization of inner flow is interpolated from a sequence of gas holdups based on images of ERT at each periods as shown Fig. 2(b).

2.2. Gas holdup

Using the conductivity data obtained from ERT, the transient gas volume fraction ($\varepsilon_{g,i}$) can be determined by applying the Maxwell relationship [17]:

$$\varepsilon_{g,i} = \frac{2\sigma_1 + \sigma_2 - 2\sigma_{mc} - \sigma_{mc}\sigma_2/\sigma_1}{\sigma_{mc} - \sigma_2/\sigma_1 + 2(\sigma_1 - \sigma_2)} \quad (1)$$

where σ_1 is the conductivity of the first phase, σ_2 the conductivity of the second phased, and σ_{mc} is the (measured) mixture conductivity. If the second phase is assumed to be non-conductive material, such as air in this study, the above equation can be simplified as

$$\varepsilon_{g,i} = \frac{2\sigma_1 - 2\sigma_{mc}}{2\sigma_1 + \sigma_{mc}} \quad (2)$$

The conductivity of the first phase (σ_1) can be measured experimentally using a conductivity meter. The local mixture conductivity (σ_{mc}) is approximately obtained using the mean value averaged from the ERT conductivity image (strictly, the Maxwell relationship is only valid for spherical particles with the same size in a low concentration and homogeneous distribution).

Following the dynamic gas disengagement technique, the gas holdup in a certain volume (e.g. for a volume with a height of H in a bubble column) within an accumulative period can be determined by Eq. (3) (H is referred as H_1 and H_2 in respect to the ERT sensing planes 1 and 2 in the later section of the paper), where m refers to the period of disengagement and N is the completion period of disengagement (Fig. 1):

$$\varepsilon_g = \sum_{i=m}^{N} \varepsilon_{g,i} \quad (m = 1,\ 2\ ,\ \ldots\ N) \quad (3)$$

Fig. 3 shows the theoretical explanation and the experimental sketch concerning Eq. (3). From Fig. 3, the plot of DGD using ERT can be divided different regions ($N = 5$), which denote different gas bubbles size, and the disengagement time from t_1 to t_5 can be obtained. Therefore, the gas holdup and the disengagement time for different bubble classes are two importance parameters in the design and scale-up of bubble columns. So the model satisfactorily describes these experimental data and provides a rational framework to predict the gas-phase behaviors in bubble column reactors.

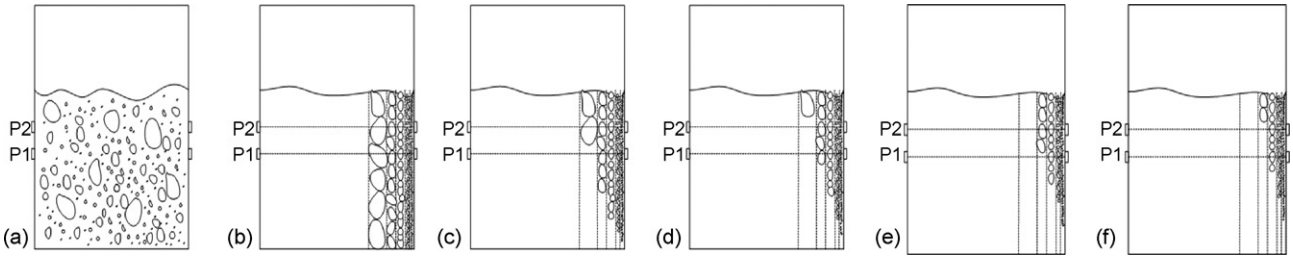

Fig. 1. Gas–liquid disengagement processes.

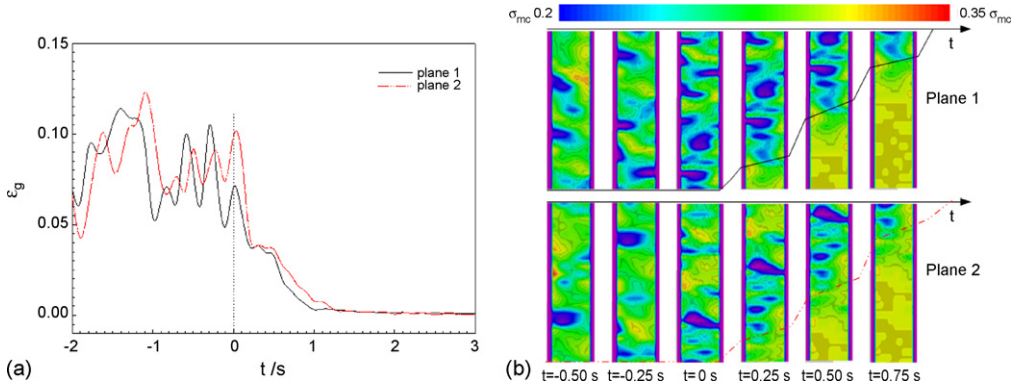

Fig. 2. (a) The bubble disengagement profiles. (b) Visualization of inner flow ($u_g = 3.4\,\mathrm{cm\,s^{-1}}$) using ERT.

2.3. Sauter bubble size and mean rise velocity

The bubble diameter and gas holdups are two vital factors with respect to the mass transfer area available in the reactor. The estimation method of bubble rise velocity and bubble size using pressure measurements have been detailed elsewhere [18]. The bubble size in the range of this study can be empirically estimated using Eqs. (4) and (5) [19,20], where d_s is the Sauter mean bubble size; D_T the column diameter; ρ_L the liquid density; ρ_g the gas density; σ_L the surface tension; ν_L the liquid kinematic viscosity; μ_L the liquid viscosity, u_g the gas superficial velocity and g is the gravitational constant:

$$\frac{d_s}{D_T} = 26\left(\frac{D_T^2 g\rho_L}{\sigma_L}\right)^{-0.5}\left(\frac{gD_T^3}{\nu_L^2}\right)^{-0.12}\left(\frac{u_g}{\sqrt{gD_T}}\right)^{-0.12} \quad (4)$$

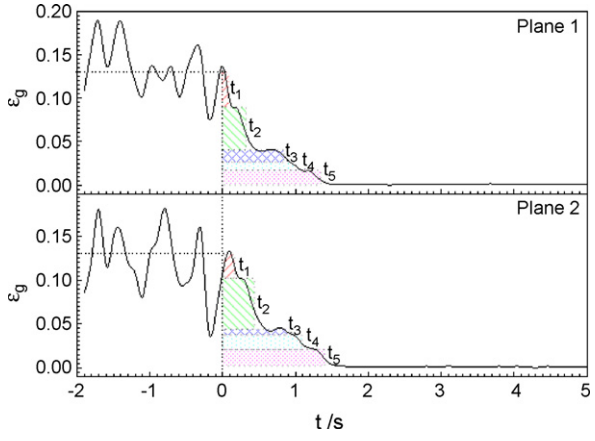

Fig. 3. The experimental sketch using the theoretical analysis ($u_g = 10.1\,\mathrm{cm\,s^{-1}}$).

$$\frac{g\rho_L d_s^2}{\sigma_L} = 38.8\left(\frac{u_g\mu_L}{\sigma_L}\right)^{-0.04}\left(\frac{\sigma_L^3\rho_L}{g\mu_L^4}\right)^{-0.12}\left(\frac{\rho_L}{\rho_g}\right)^{0.22} \quad (5)$$

Another method is developed based on the measurement obtained from ERT to estimate both the Sauter bubble size and mean rise velocity. First, we recorded the gas holdup (Eq. (3)) and the bubble rising time for disengagement period of different bubble classes. For example, the rising time for 'larger' bubbles is t_1 and similarly, the rising time for 'smaller' bubbles is t_N (refer to Fig. 4). The vertical distance above the gas distributor is H (H_1 for sensing plane 1 and H_2 for sensing plane 2 are referred in the later section). So the rise velocity of bubbles in different classes is estimated as below

$$u_{b,i} = \frac{H}{t_i} \quad (i = 1,\ 2\ ,\ \ldots\ N) \quad (6)$$

where $u_{b,i}$ is the rise velocity, H the vertical distance above the gas distributor and t_i is the bubble rising time for disengagement period of different classes bubble swarm.

With the bubble rise velocity derived by Eq. (6), the bubble sizes can be estimated by using appropriate correlation. The correlation given by Ref. [21] is used to estimate the small diameter bubbles ($d_b < 0.15$ cm) (Eq. (7)), where V_b is the volume of the bubble:

$$u_b = \frac{1}{4}\left(\frac{6\rho_L g}{\pi\mu_L}\right)^{1/3} V_b^{1/3} \quad (\text{for } d_b < 0.15\,\mathrm{cm\,s^{-1}}) \quad (7)$$

The rise velocity of large diameter bubbles in a low-viscosity media was described by Mendelson for the bubble size region

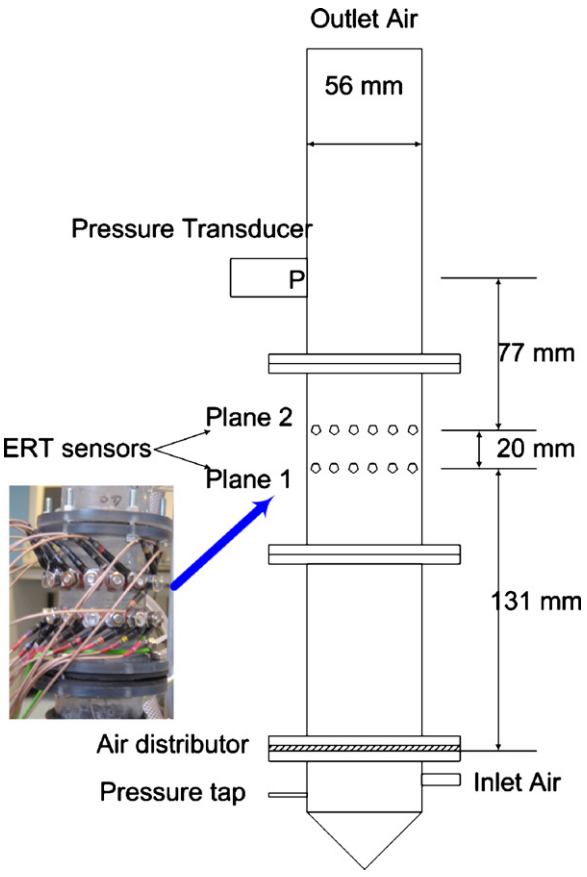

Fig. 4. The experimental setup.

from 0.2 to 8 cm (Eq. (8)) [22]:

$$u_b = \sqrt{\left(\frac{2\mu_L}{d_b \rho_L}\right) + 0.5 d_b g} \quad (\text{for } d_b \geq 0.2\,\text{cm},\ u_b > 25\,\text{cm s}^{-1}) \tag{8}$$

Finally, the Sauter mean bubble size and mean rise velocity can be expressed as

$$d_s = \frac{\sum_{i=1}^{N} \varepsilon_{g,i}}{\sum_{i=1}^{N} \varepsilon_{g,i}/d_{b,i}} \tag{9}$$

$$\bar{u}_b = \frac{\sum_{i=1}^{N} \varepsilon_{g,i} u_{b,i}}{\varepsilon_g} \tag{10}$$

2.4. The rise velocity of bubble swarm

The bubble residence-time depends on the rise velocity of bubbles. The mean rise velocity of gas bubble swarm is a function of gas velocity on the basis of the drift-flux modal [23], which is given by

$$\bar{u}_b = \frac{u_g}{\varepsilon_g} - \frac{u_L}{1-\varepsilon_g} \tag{11}$$

In this study, the liquid is operated in the batch wise, therefore, the liquid superficial velocity, $u_L = 0$.

3. Experimental

Experiments were performed using a small diameter Perspex experimental column of 1.2 m in height and 0.056 m in diameter (Fig. 4). A thermometer (Pt100) was used to provide a continuous monitoring of the water temperature. A pressure transducer was fitted into the inner wall of the column with 0.228 m above the air distributor, which was used to measure the local gage pressure in the up-column. Two rings of ERT sensors, each composed of 16 rectangular electrodes, were mounted in the inner wall of the column in a non-invasive fashion. The electrodes were made of stainless steel with a contact area of 6 mm (w) × 14 mm (h). The bottom ERT sensor ring was located 0.131 m above the air distributor. The details of the column configuration are shown in Fig. 4.

Air as the gas phase was injected into the column that filled with the mains tap water. No conductivity–temperature compensation was applied since the water temperature was monitored and maintained as about 22 °C throughout the experiment. Two types of perforated distributor with 0.003 in. thickness consisting of five holes in 1 mm diameter or in 3 mm diameter, which were arranged with an equilateral triangular pitch of 14 mm, were used as the sparger. These will be referred to as sieve-plate 1 and sieve-plate 2, respectively.

A commercially electrical resistance tomography system (P2000, Industrial Tomography System Ltd., Manchester, UK) was used for data collection. The data collection rate was 9.5 frames s^{-1} with an excitation signal frequency of 38.4 kHz.

4. Results and discussion

4.1. The comparison of using both pressure method and electrical resistance tomography

Fig. 5 shows that a comparison of using both the pressure method and ERT method to estimate the average gas holdup as a function of superficial gas velocity in the column, for two type of sparger, sieve-plate 1 and sieve-plate 2. The agreement between

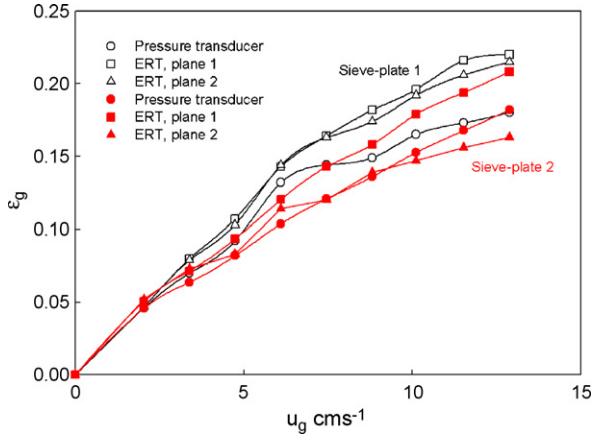

Fig. 5. Comparison of average gas holdup as a function of gas superficial velocity.

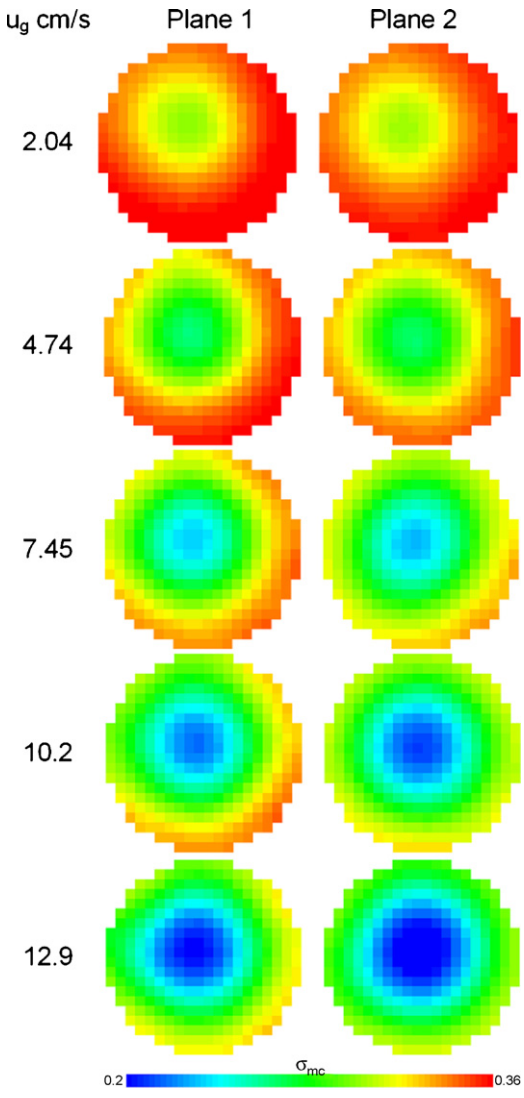

Fig. 6. The gas holdup distribution images.

results obtained by two methods is generally very good. There was a tendency ERT to predict slightly larger holdups. The slight discrepancy is likely to be the error of different measurement principles. It explains that the open area of hole will slightly affect the gas residence time and the gas distribution.

4.2. The radial distribution of holdups

The image processed from data obtained by ERT can provide the cross-sectional time-averaged gas holdup distribution at a given height. Fig. 6 shows the cross-sectional gas holdups, in color scale, of the water–air system for different superficial gas velocities. The different color regions represent gas holdups ranging from the high concentration (in blue) to low (in red). It can be seen from Fig. 6 that the higher gas concentrations at the center of lower level plane (plane 1). Further up the column (plane 2), the gas has spread radically. However, with an increase of superficial gas velocity, the color scale in the center region exchange constantly, namely there is a maximum holdup in the center of cross-section.

4.3. Holdups distribution of large bubble swarm and small bubble swarm

Fig. 7 shows the holdups distribution of large bubble swarm and small bubble swarm using both ERT method and pressure method. From Fig. 7, the values obtained from both methods are very closed. Both holdups of large bubbles and small bubbles increase with increasing superficial gas velocity in Fig. 7, which is in agreement with the experimental data reported by Krishna and Ellenberger [24] and Jin et al. [18]. The coalescence of bubbles increases with increasing superficial gas velocity, which in turn increases the holdup of large bubbles and slightly increases the holdup of small bubbles in comparison with an increase of overall gas holdup. But there is the holdup fraction of large bubble in gas velocity below 5 cm s^{-1}, which is similar to information reported in literature [23]. This possible explanation could be that the trend of gas bubble random collisions in a small diameter bubble column take place easily. Such collisions can lead to coalescence of the bubbles resulting in changes to the mean size and the size distribution of the bubbles while rising up through the column.

4.4. Rise velocity of bubble swarm

Using ERT, the mean rise velocities of bubble swarm (based on Eq. (6)) are calculated and shown in Fig. 8. Meanwhile, Eq.

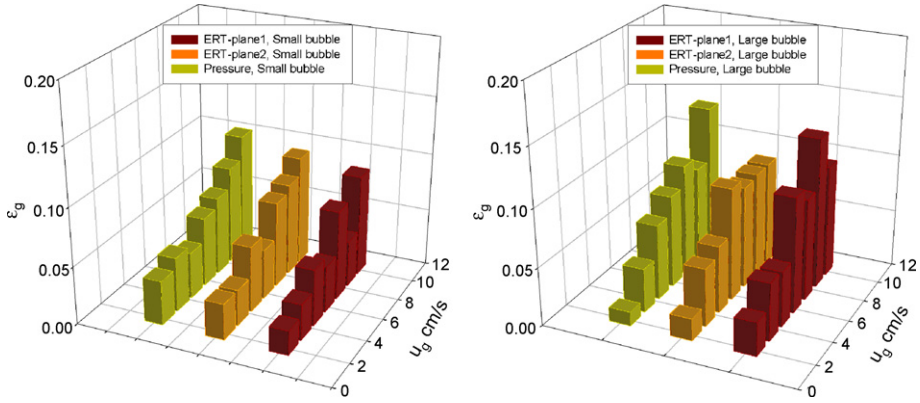

Fig. 7. The holdups distribution of large bubble swarm and small bubble swarm.

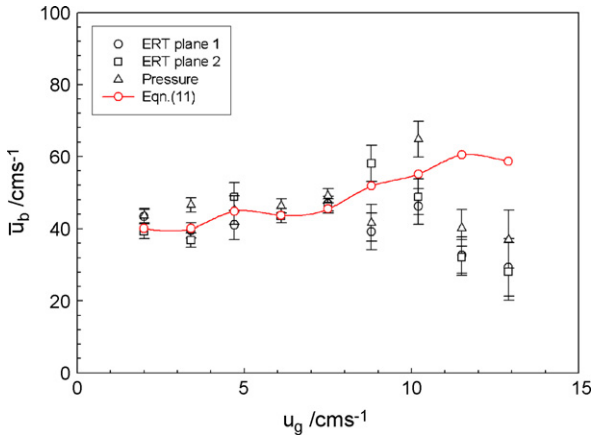

Fig. 8. The mean rise velocity of bubble swarm using ERT.

(11) is adopted to calculate the mean bubble rise velocity in order to verify the method of ERT. The experimental values are in good agreement with the values using DGD of pressure transmitter. However, when $u_g > 10\,\mathrm{cm\,s^{-1}}$, there are some errors. The reason can be explained as the flow regime changed to the slug regime [23] and the application of this method to measure the rise velocity of bubble in slug regime is not accurate.

4.5. Sauter mean bubble size

The Sauter mean bubble size estimated by Eqs. (4), (5) and (9) are shown Fig. 6. From Fig. 6, the values obtained from DGD using ERT are in good agreement with the ones using pressure transmitter. In order to verify the method, Eqs. (4) and (5) are adopted to estimate the values in the range of this study as shown Fig. 6. When $u_g < 10\,\mathrm{cm\,s^{-1}}$, the value obtained Eq. (6) in good agreement with our experimental values, but there are some errors with the value derived from Eq. (3). The reason can be explained as the Akita and Yoshida's correlation can only be used for gas feeding through single holes or pipes. When $u_g > 10\,\mathrm{cm\,s^{-1}}$, the experimental value is smaller than the values derived from Eqs. (4) and (5). Meanwhile, this can also be interpreted as due to the operation in the slug regime (Fig. 9).

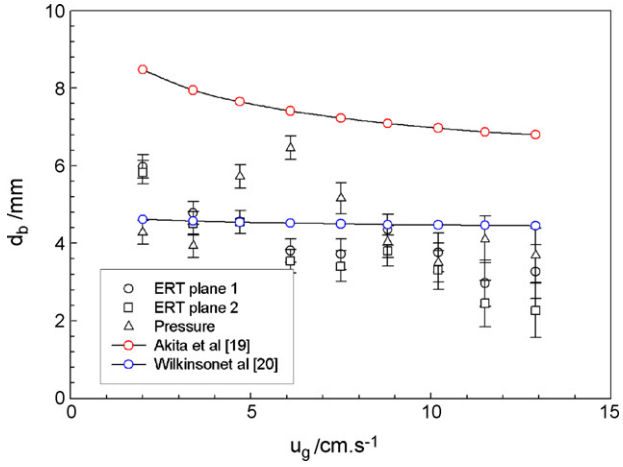

Fig. 9. The Sauter mean bubble size.

5. Conclusions

The disengagement measure gives the integral gas content as a function of time and provides a great detail of information. As different-sized bubbles at different speeds pass through the column, the disengagement technique reveals information on these aspects of bubble size distribution and rise velocity. These results are in agreement with data reported in the literature. The disengagement technique based on ERT measurement is a suitable approach for detecting the bubble behaviors in bubble columns. Using the theory and methods developed in the paper the Sauter mean bubble size and bubble rise velocity in a bubble column can be quantified. For obtaining accurate value of bubble characteristics, care in the use of ERT should be taken to ensure that experimental measurements are congruent with requirements for appropriate sampling frequency and noise levels. Further study on a large-scale bubble column is proposed to verify the proposed method of DGD using ERT at industrial scale.

The results demonstrate ERT can be used as an online monitoring tool to provide very useful information for diagnosing of the 'inside' flow behavior of bubble column reaction.

References

[1] L.S. Fan, Gas–liquid–solid Fluidization Engineering, Butterworth, Boston, 1989.
[2] M.P. Dudukovic, Opaque multiphase reactors: experimentation, modeling and troubleshooting, Oil Gas Sci. Technol. 55 (2000) 135–158.
[3] K. Sriram, R. Mann, Dynamic gas disengagement: a new technique for assessing the behaviour of bubble columns, Chem. Eng. Sci. 32 (1977) 571–580.
[4] R. Krishna, M.I. Urseanu, J. Ellenberger, Rise velocity of a swarm of large gas bubbles in liquids, Chem. Eng. Sci. 54 (1999) 171–183.
[5] C. Maretto, R. Krishna, Modeling of a bubble column slurry reactor for Fischer–Tropsch synthesis, Catal. Today 52 (1999) 279–289.
[6] S.A. Shetty, M.V. Kantak, B.G. Kelkar, Gas-phase backmixing in bubble column reactors, AIChE J. 38 (1992) 1013–1026.
[7] S.A. Patel, J.G. Daly, D.B. Bukur, Holdup and interfacial area measurements using dynamic gas disengagement, AIChE J. 36 (1990) 93–105.
[8] M. Wang, R. Mann, F.J. Dickin, Electrical resistance tomography sensing system for industrial applications, Chem. Eng. Commun. 175 (1999) 49–70.
[9] R.A. Williams, M. Wang, Dynamic imaging of process plant reactors and separators using electrical process tomography, Oil Gas Sci. Technol. 55 (2000) 185–186.
[10] M. Wang, Impedance mapping of particulate multiphase flows, Flow Meas. Instrum. 16 (2005) 183–189.
[11] E. Fransolet, M. Crine, P. Marchot, D. Toye, Analysis of gas holdup in bubble columns with non-Newtonian fluid using electrical resistance tomography and dynamic gas disengagement technique, Chem. Eng. Sci. 60 (2005) 6118–6123.
[12] E. Fransolet, M. Crine, G. L'Homme, D. Toye, Analysis of electrical resistance tomography measurements obtained on a bubble column, Meas. Sci. Technol. 21 (2001) 1055–1060.
[13] M. Wang, X. Jia, M. Bennet, R.A. Williams, Bubble column measurement and control using electrical resistance tomography, in: H. Xie, Y. Wang, Y. Jiang (Eds.), Computer Application in the Minerals Industries, A.A. Balkema/Rotterdam, Netherlands, 2001, pp. 459–464.
[14] D. Toye, E. Fransolet, D. Simon, M. Crine, G. L'Homme, P. Marchot, Possibilities and limits of application of electrical resistance tomography in hydrodynamics of bubble columns, Can. J. Chem. Eng. 83 (2005) 4–10.
[15] H. Jin, M. Wang, R.A. Williams, The effect of sparger geometry on gas bubble flow behaviours using electrical resistance tomography, Chin. J. Chem. Eng. 14 (2006) 127–131.

[16] J.G. Daly, S.A. Patel, D.B. Bukur, Measurement of gas holdups and Sauter mean bubble diameters in bubble column reactors by dynamic gas disengagement method, Chem. Eng. Sci. 47 (1992) 3647–3654.
[17] J.C. Maxwell, A Treatise on Electricity and Magnetism, Clarendon Press, Oxford, 1873.
[18] H. Jin, S. Yang, T. Zhang, Z. Tong, Bubble behaviour of a large-scale bubble column with elevated pressure, Chem. Eng. Technol. 27 (2004) 1007–1013.
[19] K. Akita, F. Yoshida, Bubble size interfacial area and liquid-phase mass transfer coefficient in bubble columns, Ind. Eng. Chem. Proc. Des. Develop. 13 (1974) 84–91.
[20] P.M. Willkinson, A.H. Haring, Mass transfer and bubble size in a bubble column under pressure, Chem. Eng. Sci. 49 (1994) 1417–1427.
[21] M. Motarjemi, G.J. Jameson, Mass transfer from very small bubbles the optimum bubble size for aeration, Chem. Eng. Sci. 33 (1978) 1415–1423.
[22] H.D. Mendelson, The prediction of bubble terminal velocities from wave theory, AIChE J. 13 (1967) 250–253.
[23] W.D. Deckwer, Bubble Column Rectors, John Wiley and Sons Ltd., New York, 1992.
[24] R. Krishna, J. Ellenberger, Gas holdup in bubble column reactors operating in the churn-turbulent flow regime, AIChE J. 42 (1996) 2627–2634.